Spin-Label Electron Spin Resonance Studies on the Mode of Anchoring and Vertical Location of the *N*-Acyl Chain in *N*-Acylphosphatidylethanolamines†

Musti J. Swamy,*,‡ M. Ramakrishnan,‡ B. Angerstein,§ and D. Marsh§

School of Chemistry, University of Hyderabad, Hyderabad 500 046, India, and Abteilung Spektroskopie, Max-Planck-Institut für biophysikalische Chemie, D-37070 Göttingen, Germany

Received March 28, 2000; Revised Manuscript Received July 5, 2000

ABSTRACT: Electron spin resonance (ESR) studies have been performed on *N*-myristoyl dimyristoylphosphatidylethanolamine (*N*-14-DMPE) membranes using both phosphatidylcholines spin-labeled at different positions in the *sn*-2 acyl chain and *N*-acyl phosphatidylethanolamines spin-labeled in the *N*-acyl chain to characterize the location and mobility of the *N*-acyl chain in the lipid membranes. Comparison of the positional dependences of the spectral data for the two series of spin-labeled lipids suggests that the *N*-acyl chain is positioned at approximately the same level as the *sn*-2 chain of the phosphatidylcholine spin-label. Further, similar conclusions are reached when the ESR spectra of the *N*-acyl PE spin-labels in dimyristoylphosphatidylcholine (DMPC) or dimyristoylphosphatidylethanolamine (DMPE) host matrixes are compared with those of phosphatidylcholine spin-labels in these two lipids. Finally, the chain ordering effect of cholesterol has also been found to be similar for the *N*-acyl PE spin-label and PC spin-labels, when the host matrix is either DMPC and cholesterol or *N*-14-DMPE and cholesterol at a 6:4 mole ratio. In both cases, the gel-to-liquid crystalline phase transition is completely abolished but cholesterol perturbs the gel-phase mobility of *N*-14-DMPE more readily than that of DMPC. These results demonstrate that the long *N*-acyl chains are anchored firmly in the hydrophobic interior of the membrane, in an orientation that is parallel to that of the *O*-acyl chains, and are located at nearly the same vertical position as that of the *sn*-2 acyl chains in the lipid bilayer. There is a high degree of dynamic compatibility between the *N*-acyl chains and the *O*-acyl chains of the lipid bilayer core, although bilayers of *N*-acyl phosphatidylethanolamines possess a more hydrophobic interior than phosphatidylcholine bilayers. These results provide a structural basis for rationalizing the biological properties of NAPEs.

N-Acyl phosphatidylethanolamines (*N*-acyl PEs, NAPEs)[1] are naturally occurring derivatives of the phospholipid phosphatidylethanolamine in which the amine of the polar headgroup is modified by acylation with long-chain fatty acids (*1*). The presence of these lipids in a variety of species such as microorganisms, plants, and animals (including fish) has been well-documented (*2*−*8*). The content of NAPEs increases dramatically when the parent tissue is subjected to a condition of stress (such as wounding in animals or dehydration of the endosperm in plant seeds), and it has been suggested that the increase in the content of NAPEs is a result of the stress-combating mechanism of the parent organisms (reviewed in ref *1*).

Considerable progress has been made in our understanding of the biosynthesis and metabolism of NAPEs in recent years. It has been shown that a membrane-bound transacylase is responsible for the *N*-acylation of phosphatidylethanolamine, resulting in the synthesis of NAPE (*1*, *9*, *10*). The NAPEs are also catabolyzed by a phospholipase D type enzyme, resulting in the production of *N*-acylethanolamines (NAEs) (see ref *11*). NAEs have been shown to exhibit a variety of properties that are of biological and medical interest. For example, anandamide (*N*-arachidonylethanolamine) and *N*-palmitoylethanolamine have been shown to act as endogenous agonists for the cannabinoid receptors type 1 and type 2, respectively (*12*, *13*), whereas *N*-oleoylethanolamine is a potent inhibitor of ceramidase (*14*). Anandamide also inhibits gap junction conductance and reduces sperm fertilizing capacity (*15*, *16*). In addition, various NAEs exhibit antibacterial, antiviral, and antineoplastic activities (reviewed in ref *1*). In view of these observations, it has been proposed that NAPEs primarily serve as precursors for the synthesis of NAEs, which then act as second messengers (*1*, *11*).

Besides the interest generated in their biological and medicinal properties, NAPEs are also studied because of their

† This work was supported in part by a research grant from the Department of Science and Technology, Government of India to M.J.S. M.R. is a Senior Research Fellow of the CSIR, Government of India.

* To whom correspondence should be addressed: School of Chemistry, University of Hyderabad, Hyderabad 500 046, India. Telephone: +91-40-301-0500 to 0510, ext. 4807. Fax: +91-40-301-2460/0145. E-mail: mjssc@uohyd.ernet.in.

‡ University of Hyderabad.

§ Max-Planck-Institut für biophysikalische Chemie.

[1] Abbreviations: PC, phosphatidylcholine; PE, phosphatidylethanolamine; NAPE or *N*-acyl PE, *N*-acyl phosphatidylethanolamine; NAE, *N*-acylethanolamine; ESR, electron spin resonance; DMPC, 1,2-dimyristoyl-*sn*-glycero-3-phosphocholine; DPPC, 1,2-dipalmitoyl-*sn*-glycero-3-phosphocholine; DMPE, 1,2-dimyristoyl-*sn*-glycero-3-phosphoethanolamine; DPPE, 1,2-dipalmitoyl-*sn*-glycero-3-phosphoethanolamine; *N*-14-DMPE, 1,2-dimyristoyl-*sn*-glycero-3-*N*-myristoylphosphoethanolamine; *N*-16-DPPE, 1,2-dipalmitoyl-*sn*-glycero-3-*N*-palmitoylphosphoethanolamine; *n*-SASL, *n*-(4,4-dimethyloxazolidine-*N*-oxyl)stearic acid; *n*-PCSL, 1-acyl-2-[*n*-(4,4-dimethyloxazolidine-*N*-oxyl)stearoyl]-*sn*-glycero-3-phosphocholine; *n*-NAPESL, 1,2-dipalmitoyl-*sn*-glycero-3-[*N*-*n*-(4,4-dimethyloxazolidine-*N*′-oxyl)stearoyl]-phosphoethanolamine; Hepes, *N*-(2-hydroxyethyl)piperazine-*N*′-2-ethanesulfonic acid.

10.1021/bi000699l CCC: $19.00
Published on Web 09/14/2000

reported membrane stabilizing property. Recent reports indicate that *N*-acyl egg PE and *N*-palmitoyl DPPE (*N*-16-DPPE) stabilize liposomes against leakage (*17*, *18*). NAEs have been reported to stabilize bilayer structure in the sense of inhibiting inverted hexagonal phase formation (*19*). *N*-16-DPPE stabilizes liposomes even in the presence of human serum, indicating that NAPEs may potentially be useful in developing liposomal formulations for drug delivery applications (*18*).

In *N*-acyl PEs isolated from natural sources, the *N*-acyl chain is usually long, the most predominant chains being palmitoyl and stearoyl (*7*, *20*). Biophysical studies (reviewed in ref *21*) have shown that, for NAPEs with long *N*-acyl chains, the *N*-acyl chain folds back into the hydrophobic interior of the membrane (*22*). Studies employing differential scanning calorimetry, ^{31}P NMR, and infrared spectroscopy, in which the *N*-acyl chain has been systematically varied while keeping the *O*-acyl chain length constant (16 C atoms), have revealed that if the length of the *N*-acyl chain is around 10 C atoms or longer, then it is firmly anchored into the membrane, whereas a chain six carbon atoms in length does not interact with the hydrophobic portion of the lipid bilayer (*22*−*24*). Also, it has been shown by attenuated total reflection (ATR) infrared spectroscopy that the *N*-palmitoyl chain of *N*-16-DPPE is oriented parallel to the *O*-acyl chains, whereas the *N*-hexyl chain of *N*-6-DPPE is randomly oriented (*25*). Another problem that has been investigated is whether the headgroup-attached *N*-acyl chains pack in a manner similar to that of the glycerolipid *O*-acyl chains. Calorimetric studies on NAPEs with matched *N*- and *O*-acyl chains have shown that the contribution of the *N*-acyl chain to the chain-melting enthalpy of the lipid is considerably smaller than that of the *O*-acyl chains, suggesting that the packing of the *N*-acyl chains differs from that of the *O*-acyl chains (*26*).

A further important aspect of the chain packing in *N*-acyl PEs regards the vertical location of the *N*-acyl chains, and especially their mobility, relative to the *O*-acyl chains. Though both *O*-acyl chains of phospholipids are attached to the glycerol backbone, X-ray and neutron diffraction studies reveal that the vertical location of the *sn*-1 and *sn*-2 chains differs with respect to the bilayer plane, the *sn*-2 chain being located one or two methylene groups higher with respect to the *sn*-1 chain (*27*, *28*). Because the *N*-acyl chains of NAPEs are attached to the phospholipid headgroup, and not to the glycerol backbone, it is possible that their positions are different with respect to the *O*-acyl chains and also that their mobilities differ from that of the *O*-acyl chains in fluid membranes. In this study, we have addressed these basic questions by using ESR spectroscopy, together with different synthetic *N*-acyl phosphatidylethanolamine derivatives that are site-specifically spin-labeled in their *N*-acyl chain. The results indicate that, despite their unconventional mode of attachment, both the bilayer environment and the segmental mobility of the *N*-acyl chains are very similar to those of the *sn*-2 *O*-acyl chains. Further, it is found that the *N*-acyl chains respond to the presence of cholesterol in the membrane in a manner very similar to that of the *sn*-2 acyl chains. These findings are consistent with the proposal that *N*-acyl PEs function as a membrane-compatible reservoir for the potentially more membrane disruptive NAEs,[2] which are only mobilized from the parent reservoir under conditions of membrane stress.

MATERIALS AND METHODS

Materials. DMPC, DPPE, and DMPE were purchased from Avanti Polar Lipids (Alabaster, AL). Myristic acid and oxalyl chloride were obtained from Fluka (Buchs, Switzerland). Cholesterol was from Sigma (St. Louis, MO). *N*-Myristoyl dimyristoylphosphatidylethanolamine was synthesized by the reaction of myristoyl chloride with DMPE as described previously (*26*).

Spin-Labels. Phosphatidylcholine spin-labels, *n*-PCSL, and stearic acid spin-labels, *n*-SASL, were synthesized according to the procedures described in ref *29*. *N*-Acyl phosphatidylethanolamine spin-labels, *n*-NAPESL, bearing the spin-label at different positions in the *N*-acyl chain were synthesized by coupling spin-labeled fatty acids, *n*-SASL, with dipalmitoylphosphatidylethanolamine (DPPE) in the presence of 1,1′-dicarbonylimidazole. A typical procedure followed for the synthesis of 8-NAPESL is given below. Forty milligrams of 8-SASL and 18 mg of dicarbonylimidazole were dissolved in a few milliliters of toluene, and the mixture was stirred at room temperature for 30 min. Thirty-five milligrams of DPPE was added, and the mixture was stirred for a further period of 30 min. The solvent was then removed by rotary evaporation; small glass beads were added, and the reaction flask was evacuated. The reaction mixture was stirred at 50 °C overnight and then checked by thin-layer chromatography. It was found that all the DPPE had reacted, and the reaction was stopped. The product mixture was dissolved in a small volume of CH_2Cl_2, and 10 volumes of acetone was added. Incubation at −20 °C overnight yielded the 8-NAPESL as a precipitate, which was separated by filtration. The purity of the product was verified by thin-layer chromatography with a chloroform/methanol/ammonium hydroxide (65:25:4; v/v) solvent system.

Sample Preparation. Samples for ESR spectroscopy were prepared in the following manner. Approximately 2 mg of the appropriate lipid was dissolved in dichloromethane, and 1 mol % spin-label was added from a 1 mg/mL stock solution in the same solvent. The solvent was then evaporated under a stream of dry nitrogen gas. Mixtures of DMPC, DMPE, and *N*-14-DMPE with cholesterol and 1 mol % spin-label were also prepared in a similar manner. The residual solvent was then removed by vacuum desiccation for a minimum of 3 h, and the lipid film was hydrated with 10 mM Hepes and 1 mM EDTA (pH 7.4). After mild vortexing, the sample was transferred to a 100 μL (1 mm outside diameter) glass capillary and pelleted by centrifugation in a benchtop centrifuge. After removal of the supernatant, the capillary was flame-sealed.

ESR Spectroscopy. ESR spectra were recorded on a Varian E-12 Century line 9 GHz ESR spectrometer. Samples in sealed 100 μL (1 mm outside diameter) glass capillaries were placed in a standard 4 mm quartz ESR tube containing light silicone oil for thermal stability. The temperature of the

[2] We have observed that at high concentrations in a DPPC host matrix, *N*-palmitoylethanolamine results in phase separation, whereas *N*-14-DMPE mixes well with DMPC at high concentrations (M. Ramakrishnan, D. Marsh, and M. J. Swamy, unpublished observations).

samples was regulated by blowing thermostated nitrogen gas through a quartz dewar that accommodated the sample tube. The sample temperature was monitored with a fine-wire thermocouple located close to the sample, at the top of the microwave cavity. Spectra were analyzed in terms of the outer hyperfine splitting, $2A_{max}$, between the spectral extrema. In general, A_{max} is dependent on both the amplitude (i.e., order) and rate of chain rotational motion, and is a useful parameter in both gel- and fluid-phase membranes. In the fluid phase, the polarity-dependent isotropic hyperfine splitting constant was calculated according to

$$a_o = {}^1/_3(A_{||} + 2A_{\perp}) \quad (1)$$

where $A_{||}$ and $A_{\perp}$ are the principal hyperfine tensor elements. They are given by $A|| = A_{max}$ and $A_{\perp} = A_{min} + 0.85$ G (*30*), where the inner hyperfine splitting is $2A_{min}$. These measurements are made at a sufficiently high temperature (60−70 °C) that slow-motional effects do not contribute, and the values calculated for a_o are not temperature-dependent (see ref *31*).

RESULTS AND DISCUSSION

Although previous studies have indicated that when the *N*-acyl chain of *N*-acyl PE is sufficiently long it can fold back and interact with the hydrophobic interior of the lipid membrane (*22*−*24*), there has been no direct demonstration that the long *N*-acyl chain is located in the hydrophobic interior of the membrane bilayer. Also, the vertical location of the *N*-acyl chain in the membrane, relative to the *O*-acyl chains, has not been investigated so far. In this study, this aspect has been investigated by spin-label ESR spectroscopy, employing phosphatidylcholines spin-labeled at different positions in the *sn*-2 acyl chain and *N*-acyl phosphatidylethanolamines spin-labeled in the *N*-acyl chain. By systematically varying the position of spin-labeling, we have determined the vertical location of the *N*-acyl chain relative to that of the *O*-acyl chains of the glycerophospholipid bilayer, and also have characterized its segmental mobility and interactions with cholesterol.

Phosphatidylcholine, Phosphatidylethanolamine, and N-Acyl Phosphatidylethanolamine Bilayers. ESR spectra of the positional isomers of *n*-NAPESL recorded in the fluid phase of DMPC, DMPE, and *N*-14-DMPE host matrixes are given in Figure 1. For comparison, the spectra of corresponding positional isomers of *n*-PCSL are also shown with dotted lines. For each host matrix, the *n*-NAPESL and *n*-PCSL spectra are qualitatively very similar at each position, *n*, of chain labeling, suggesting that the spin-labels attached on the *N*-acyl chain of NAPE and the *sn*-2 chain of PC experience very similar environments and have comparable segmental motions. This implies that the *N*-acyl chain of NAPE and *sn*-2 (*O*-) acyl chain of PC are located at approximately the same depth from the membrane interface. However, minor differences can be noticed in several cases. Most notably, in almost all cases, the outer peaks in the spectra of *n*-NAPESL are slightly more separated, indicating that the hyperfine anisotropy is somewhat larger than for *n*-PCSL.

The temperature dependence of the outer hyperfine splitting, $2A_{max}$, for the *n*-PCSL and *n*-NAPESL spin-labels in the different host matrixes is given in panels A−E of Figure 2. Two important pieces of information can be deduced from these data. First, the values of $2A_{max}$ for the *n*-NAPESL spectra are higher than those for the *n*-PCSL spectra at all temperatures throughout the fluid phase of DMPE and *N*-14-DMPE host membranes. Second, the values of $2A_{max}$ exhibit somewhat steeper temperature gradients for the *n*-PCSL spin-labels than for the *n*-NAPESL spin-labels, in all the three host matrixes. This holds for spin-label positions close to the headgroup region (Figure 2A−C), whereas for spin-label positions close to the methyl end of the acyl chains (Figure 2D,E), the temperature gradients for both types of spin-labels become rather similar. In DMPC, the relative values of A_{max} for the *n*-NAPESL and *n*-PCSL spin-labels switch from the former being greater up to $n = 10$ (Figure 2A−C) to the latter being greater for $n = 12$ and 14 (Figure 2D,E). The segmental mobility of *n*-NAPESL therefore becomes greater than that of *n*-PCSL for $n \geq 12$.

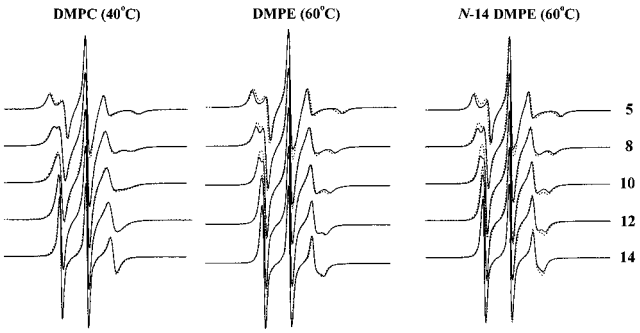

FIGURE 1: ESR spectra of phosphatidylcholine and *N*-acyl phosphatidylethanolamine spin-labels in DMPC, DMPE, and *N*-14-DMPE membranes: (—) *n*-NAPESL *N*-acyl PE spin-label and (···) *n*-PCSL phosphatidylcholine spin-label. The spin-label position, *n*, in the *sn*-2 chain for PC spin-labels or in the *N*-acyl chain for the *N*-acyl PE spin-labels is indicated on the right of the figure. The temperature at which the spectra were recorded is indicated for each panel separately. The buffer included 10 mM Hepes and 1 mM EDTA (pH 7.4). The spectral width is 100 G.

The differences in the temperature dependences of $2A_{max}$ for *n*-NAPESL and *n*-PCSL demonstrate that, at positions closer to the headgroup (C-5 and C-8, and to a somewhat lesser degree C-10), the *N*-acyl chain is less mobile than the *O*-acyl chains, in all the three host lipids (see Figure 2A−C). These results reflect the reduced transition enthalpy and entropy contributed by the *N*-acyl chain of NAPEs, as deduced earlier from DSC studies (*26*).

Phosphatidylcholine and N-Acyl Phosphatidylethanolamine Bilayers with Cholesterol. It is well-known that cholesterol exhibits an ordering effect on the chains of diacyl phospholipids in the fluid phase. At temperatures in the vicinity of the gel-to-fluid phase transition and below, cooperative chain melting is abolished by addition of cholesterol and the liquid-ordered phase is formed (*32*). When the mole fraction of cholesterol in the mixture is sufficiently high, only the liquid-ordered phase is observed. For DPPC, this occurs when the cholesterol fraction is greater than about 35 mol % (*33*). These highly characteristic effects of cholesterol on chain mobility and ordering afford a further method of investigating the mode of integration of the *N*-acyl chains in the bilayer lipid membrane.

The temperature dependences of $2A_{max}$ for the 5-PCSL and 5-NAPESL spin-labels in DMPC and *N*-14-DMPE membranes, with and without 40 mol % cholesterol, are given in

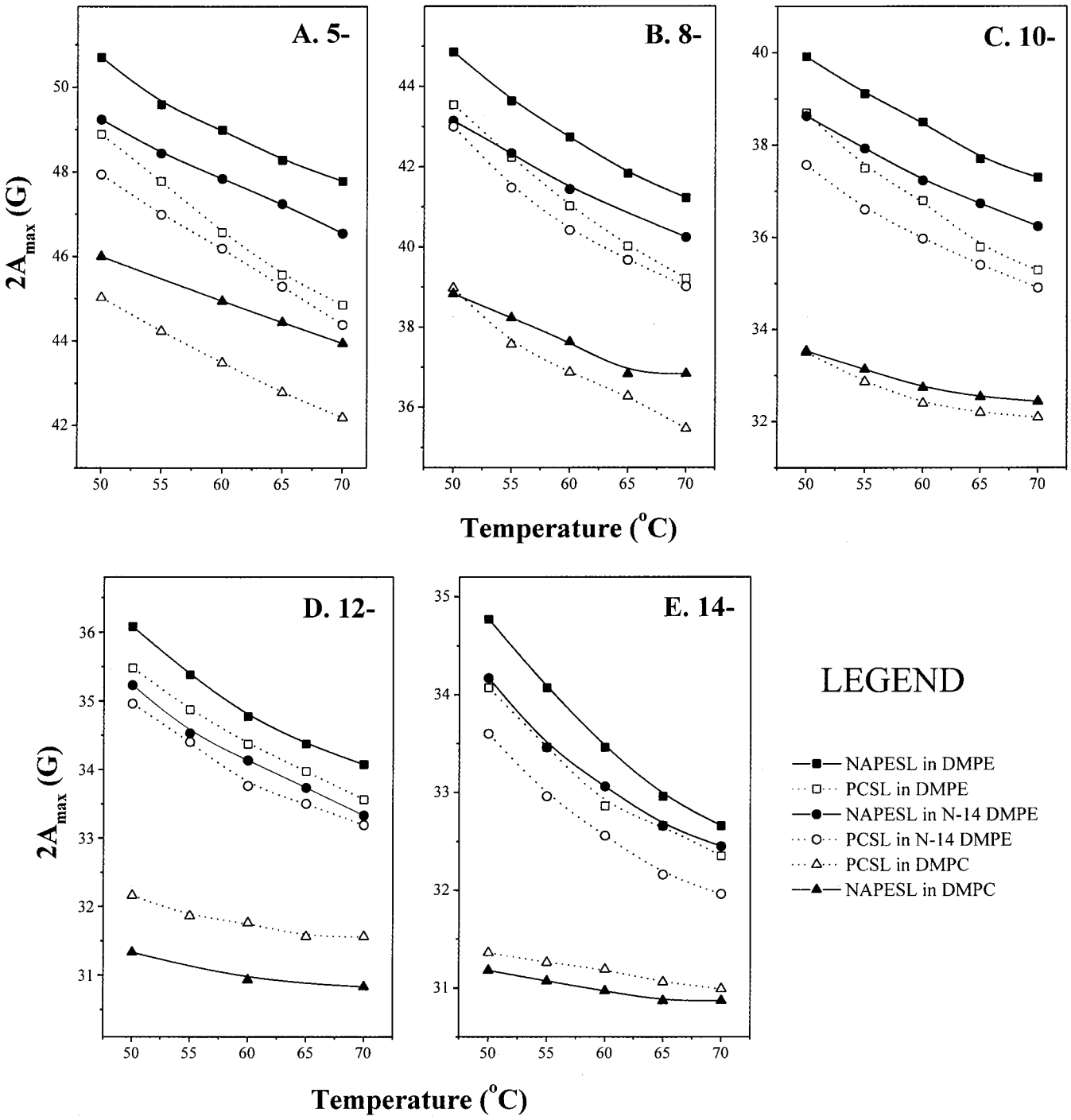

FIGURE 2: Temperature dependence of the outer hyperfine splittings, $2A_{max}$, for *n*-NAPESL (black symbols) and *n*-PCSL (white symbols) spin-labels in DMPC (triangles), DMPE (squares), and *N*-14-DMPE (circles) membranes: (A) 5-PCSL (white symbols) and 5-NAPESL (black symbols), (B) 8-PCSL (white symbols) and 8-NAPESL (black symbols), (C) 10-PCSL (white symbols) and 10-NAPESL (black symbols), (D) 12-PCSL (white symbols) and 12-NAPESL (black symbols), and (E) 14-PCSL (white symbols) and 14-NAPESL (black symbols).

panels A and B of Figure 3, respectively. For both the spin-labels in DMPC membranes, values of $2A_{max}$ decrease relatively slowly in the gel phase and throughout the pretransition region, as the temperature is raised from 1 to 23 °C. Increasing the sample temperature to 25 °C results in an abrupt drop in the value of $2A_{max}$, at the chain-melting phase transition of DMPC (23 °C; *34*), whereas a further increase in temperature up to 40 °C results in only a steady decrease in the value of $2A_{max}$ (Figure 3A). Similarly, in *N*-14-DMPE membranes, the values of $2A_{max}$, for both 5-PCSL and 5-NAPESL, change only slowly between 20 and 45 °C, but decrease steeply between 45 and 50 °C, which corresponds to chain melting of the *N*-acyl lipid that is seen at around 51 °C by calorimetry (*26*). Above this temperature, the outer hyperfine splittings decrease in a more gradual manner, as the temperature is increased up to 70 °C in the fluid phase (Figure 3B).

Even though, overall, the segmental mobility of the *N*-acyl chain is comparable to that of the *sn*-2 acyl chains, the mobility of the two chains differs significantly in both the fluid and gel phases of *N*-14-DMPE. The values of A_{max} for 5-NAPESL are smaller in the gel phase, and larger in the

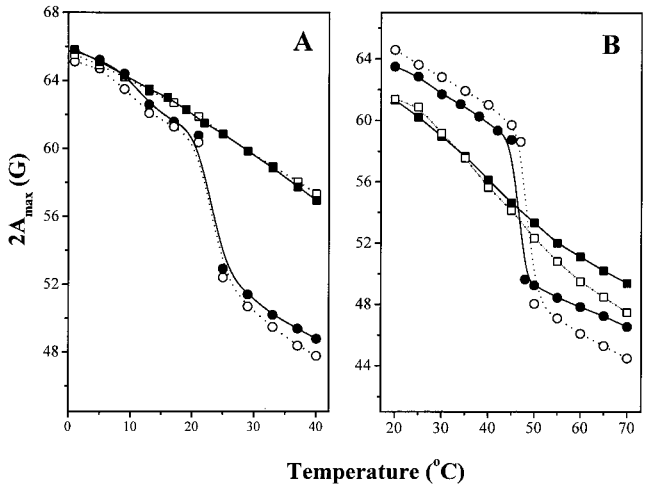

FIGURE 3: Temperature dependence of the outer hyperfine splittings, $2A_{max}$, for 5-PCSL (○ and □) and 5-NAPESL (● and ■) spin-labels in different lipid host membranes: (A) DMPC (● and ○) and DMPC/cholesterol (6:4 mole ratio, ■ and □) host membranes and (B) *N*-14-DMPE (● and ○) and *N*-14-DMPE/cholesterol (6:4 mole ratio, ■ and □) host membranes.

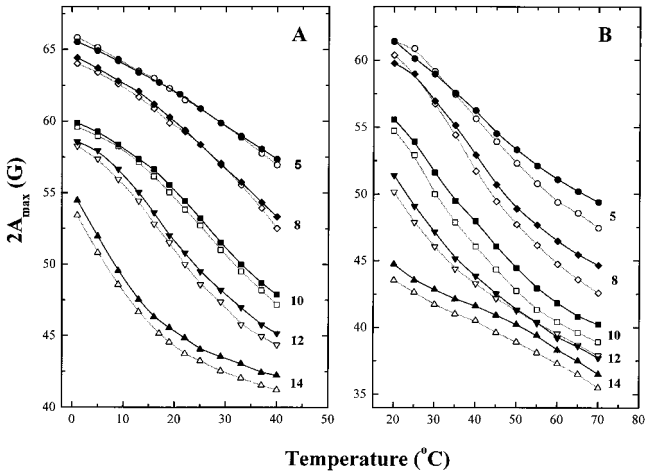

FIGURE 4: Temperature dependence of the outer hyperfine splittings, $2A_{max}$, for *n*-NAPESL (solid lines and black symbols) and *n*-PCSL (dotted lines and white symbols) spin-labels in (A) DMPC/cholesterol (6:4 mole ratio) and (B) *N*-14-DMPE/cholesterol (6:4 mole ratio) host membranes. The spin-label position, *n*, is indicated on the figure for each curve.

fluid phase, than those of 5-PCSL (Figure 3B). Correspondingly, the total change in A_{max} on chain melting of *N*-14-DMPE bilayers is smaller for 5-NAPESL than for 5-PCSL. The spin-label measurements therefore indicate that the *N*-acyl chains are less well packed in the gel phase, and are more ordered in the fluid phase, than are the *O*-acyl chains. This result also is in agreement with previous calorimetric studies, which show that the contribution of the *N*-acyl chain to the chain-melting enthalpy and entropy of *N*-acyl PEs is smaller than that of the *O*-acyl chains (*26*).

Addition of 40 mol % cholesterol abolishes the chain-melting phase transition of both DMPC and *N*-14-DMPE membranes (Figure 3A,B). The outer hyperfine splittings of the chain-labeled lipids then decrease monotonically with increasing temperature, throughout the entire range that was studied. Whereas the effects of 40 mol % cholesterol differ in detail between DMPC and *N*-14-DMPE bilayers (Figure 3A,B), in both lipid hosts the chains are more ordered than in the fluid phase of bilayers without cholesterol. Thus, cholesterol induces the formation of the liquid-ordered phase not only for phosphatidylcholines, which is well-characterized (*35*), but also for the three-chain *N*-acyl PE lipids (see Figure 3B). Significantly, these effects are felt almost equivalently by the 5-NAPESL and 5-PCSL spin-labels, in both host lipids. This demonstrates that the *N*-acyl chain experiences interactions with cholesterol that are similar to those for the *O*-acyl chains. The difference in cholesterol interactions with the *N*-acyl PE, as compared with those with phosphatidylcholine, is that bilayers of the former undergo a considerably larger perturbation of the chain mobility at gel-phase temperatures. This may be related to the enhanced mobility of the *N*-acyl chain, relative to the *O*-acyl chain, in bilayers of *N*-14-DMPE alone (Figure 3B). It is not entirely surprising that the three-chain *N*-acyl PEs, which are also negatively charged, differ somewhat in their interactions with cholesterol, as compared with diacyl phosphatidylcholines.

The temperature dependences of $2A_{max}$ for the different *n*-PCSL and *n*-NAPESL positional isomers in DMPC/cholesterol (6:4 mole ratio) and in *N*-14-DMPE/cholesterol (6:4 mole ratio) membranes are given in panels A and B of Figure 4, respectively. From these figures, it is apparent that both *n*-NAPESL and *n*-PCSL spin-probes exhibit very similar temperature dependences at each labeling position, in either host matrix. In DMPC/cholesterol (6:4 mole ratio) membranes, the mobility of the *n*-NAPESL spin-labels is very similar to that of the *n*-PCSL spin-labels, also for chain segments labeled deeper in the membrane than the $n = 5$ position. At these chain positions, the fluidizing effect of cholesterol in the gel phase becomes quite marked, as already found at the $n = 5$ position in *N*-14-DMPE (Figure 3B). This consistency shows that, throughout its entire length, the *N*-acyl chain of *n*-NAPESL experiences the same interactions with cholesterol as does the *sn*-2 chain of *n*-PCSL. Similar conclusions may be drawn from the corresponding measurements in *N*-14-DMPE/cholesterol (6:4 mole ratio) membranes. The differences between *n*-NAPESL and *n*-PCSL are somewhat greater, in the latter case, and the difference in interactions of *N*-14-DMPE and DMPC with cholesterol is maintained throughout the chain-labeling positions.

Chain Segmental Mobility Profiles. The outer hyperfine splitting constants obtained for different positional isomers, *n*, of *n*-PCSL and *n*-NAPESL, recorded at a temperature above the chain-melting transition in different host matrixes, with and without cholesterol, are given in panels A−E of Figure 5. There is very little difference in the values of $2A_{max}$ for given positional isomers (*n*) of *n*-PCSL and *n*-NAPESL in the DMPC host matrix, but in DMPE and in *N*-14-DMPE host matrixes, the ESR spectra of *n*-NAPESL exhibit values of $2A_{max}$ slightly higher than those of *n*-PCSL, at all chain positions (Figure 5A−C). A similar result is obtained for the cholesterol-containing systems (Figure 5D,E), even though the profiles are shifted to considerably higher values of A_{max} because of the chain ordering by cholesterol. The consistently higher values of $2A_{max}$ for NAPESL indicate that the nitroxide labels attached to the *N*-acyl chains exhibit a lower degree of mobility, especially of segmental motion. This suggests that the C atoms in the *N*-acyl chains of this lipid may be located at a slightly higher vertical position, as compared with the corresponding C atoms of the *sn*-2 chain of *n*-PCSL. It is estimated from the data on A_{max} that the

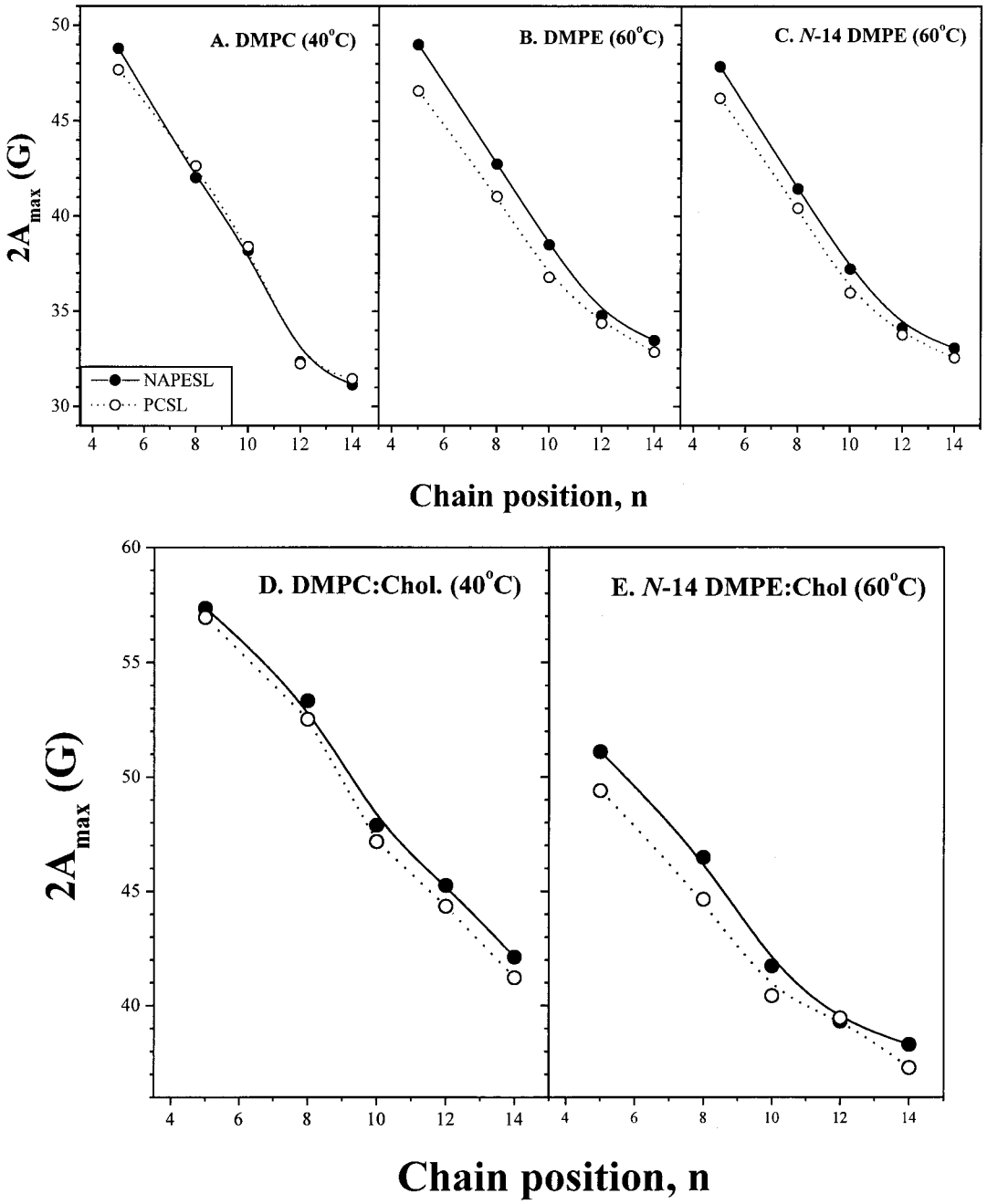

FIGURE 5: Outer hyperfine splittings, $2A_{max}$, as a function of the position, *n*, of chain labeling for *n*-NAPESL (●) and *n*-PCSL (○) in the fluid phase of (A) DMPC, (B) DMPE, (C) *N*-14-DMPE, (D) DMPC/cholesterol (6:4 mole ratio), and (E) *N*-14-DMPE/cholesterol (6:4 mole ratio) host matrixes. The temperature at which the spectra were recorded is indicated on each panel.

N-acyl chain lies approximately 0.8 and 0.6 CH_3 unit higher than the *sn*-2 chain in DMPE and *N*-14-DMPE, respectively.

Transmembrane Polarity Profiles and Chain Location. The positional profiles of the isotropic hyperfine splitting constant, a_o, obtained from eq 1, are given in panels A−E of Figure 6, for the *n*-NAPESL and *n*-PCSL spin-labels in DMPC, DMPE, and *N*-14-DMPE host membranes as well as in DMPC and *N*-14-DMPE membranes containing 40 mol % cholesterol. The gradient of decreasing polarity with increasing position, *n*, toward the center of the membrane is clearly discerned in each case. For all the five host matrixes, the values of a_o are somewhat larger for the *n*-NAPESL spin-labels than for the corresponding *n*-PCSL spin-labels. Further, it is seen that the values of a_o for the spin-labels bearing the nitroxide moiety toward the methyl end of the chain are considerably lower in the *N*-14-DMPE host matrix, as compared to DMPC and DMPE host matrixes (Figure 6A−C). This is also the case for both cholesterol-containing systems (Figure 6D,E), relative to DMPC and DMPE.

Unlike A_{max}, the isotropic hyperfine splitting constant, a_o, is sensitive only to the polarity of the local environment at the position of the spin-label (see ref *36*). Its value does not depend on the segmental mobility of the chain. The positional profiles of a_o that are given for *n*-NAPESL and *n*-PCSL in Figure 6 are displaced relatively by 0.5−1 CH_2 unit for DMPC, by ca. 0.5 CH_2 unit for DMPE, and by 0.5−1.1 CH_2 units for *N*-14-DMPE. In DMPC/cholesterol (6:4 mole ratio) and *N*-14-DMPE/cholesterol (6:4 mole ratio) membranes, the corresponding relative vertical displacements are approximately 0.6 and 1.0 CH_2 unit, respectively. These displace-

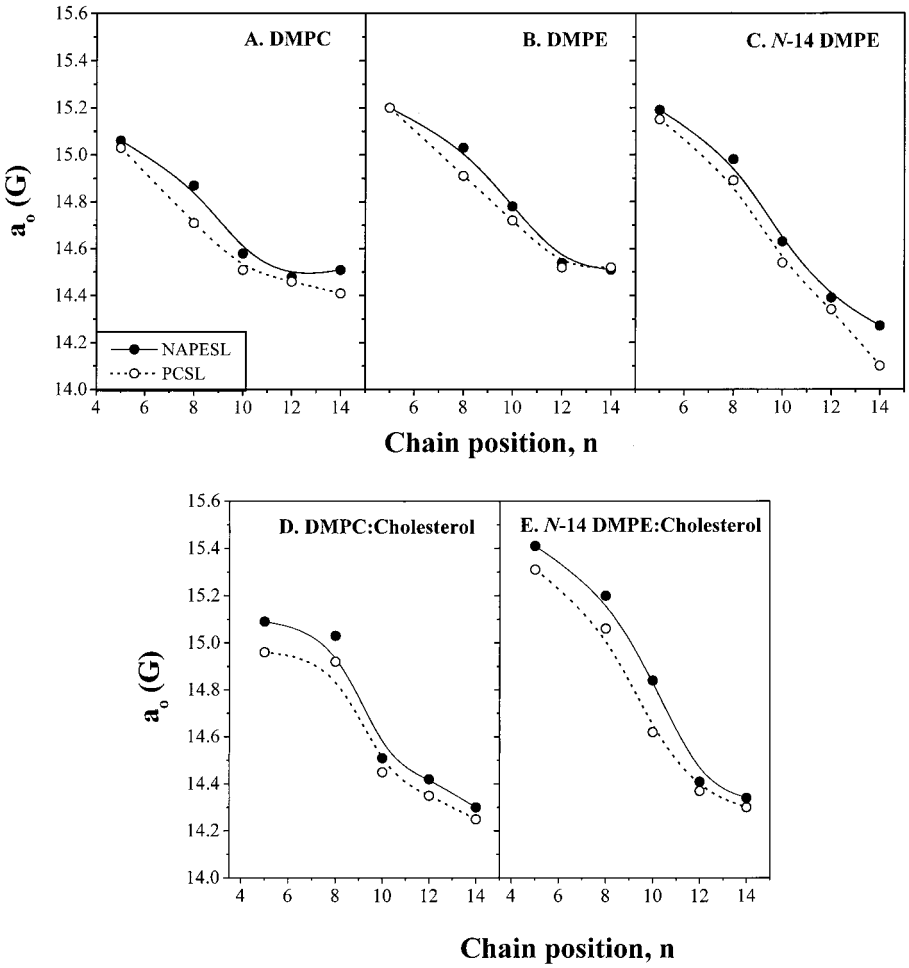

FIGURE 6: Plots of the isotropic hyperfine splitting constant, a_o, as a function of the spin-label position, *n*, for *n*-NAPESL (●) and *n*-PCSL (○) spin-labels in (A) DMPC, (B) DMPE, (C) *N*-14-DMPE, (D) DMPC/cholesterol (6:4 mole ratio), and (E) *N*-14-DMPE/cholesterol (6:4 mole ratio) membranes.

ments are broadly consistent with those deduced from the profiles of A_{max}. The approximate consistency of the two sets of shifts implies not only that the *N*-acyl and *sn*-2 chains are situated at rather similar vertical locations but also that the segmental mobilities of the chains in the same location are rather similar. The *N*-acyl chains are therefore accommodated in fluid lipid membranes in a manner that is fully compatible with the dynamic *O*-acyl chain environment of the bilayer core. This is a very significant result, in view of the very different mode and position of attachment, relative to the polar headgroup, of the *N*-acyl and *O*-acyl chains. A schematic diagram of *N*-14-DMPE, depicting the relative orientation of the *N*-acyl chain with respect to the *O*-acyl chains, deduced from the ESR studies presented here, is given in Figure 7.

Interestingly, toward the methyl end of the chain, the values of a_o are considerably smaller in the *N*-14-DMPE host matrix than in DMPC and DMPE host matrixes, for both spin-labels. The absolute values, in *N*-14-DMPE, are close to those found in a completely apolar hydrocarbon environment, such as that of *n*-decane (*37*). This indicates that the interior of the *N*-14-DMPE membranes is considerably more hydrophobic than those of DMPC and DMPE membranes. A comparable situation is found in membranes containing equimolar cholesterol (*38*) and also in the membranes with 40 mol % cholesterol in this study (Figure 6D,E). Thus, introduction of the third *N*-acyl chain in the bilayer core of

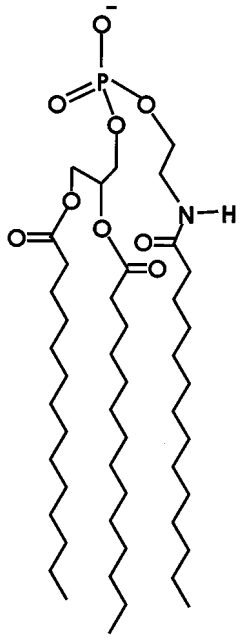

FIGURE 7: Schematic diagram of *N*-14-DMPE, indicating the relative disposition of the *N*-acyl chain with respect to the *O*-acyl chains.

N-14-DMPE, although not affecting the lipid chain dynamics very dramatically, does, nevertheless, have a considerable

effect on the polarity at the center of the membrane. The height of the hydrophobic barrier is increased, and correspondingly, the degree of water penetration into the middle of the membrane is decreased, although it may conceivably be increased somewhat in the outer regions of the membrane.

Functional Implications of N-Acylation. As outlined in the introductory section, the content of NAPEs and NAEs increases dramatically when the parent organism is subjected to a condition of stress (*1*, *11*). NAPEs serve as precursors for NAEs, which have been shown to act as neurotransmitters and second messengers. In addition, NAPEs have been demonstrated to modulate the activity of membrane-bound enzymes. Conversion of zwitterionic PE, by *N*-acylation, to the negatively charged NAPE resulted in an inactivation of the Ca^{2+}-ATPase from the sarcoplasmic reticulum (*39*). In another study, the activity of delipidated and solubilized lysosomal β-glucocerebrosidase from rat liver was found to be activated by *N*-acyl dioleoyl PEs, and their stimulatory power increased with increasing *N*-acyl chain length (*40*). Though the *N*-acyl chain length dependence on the activity of the phospholipase D type enzyme that catalyzes the conversion of NAPE to PA and NAE has not been characterized, it has been shown that in both animal and plant tissues the enzyme is membrane-bound and does not act upon PC or PE (*41*, *42*). This is in contrast to the normal, soluble phospholipase D enzymes, and suggests that the NAPE-specific enzyme probably requires the long *N*-acyl chain, which (as found here) is embedded in the hydrophobic interior of the membrane, for its substrate.

Recent studies on neuronal cells indicate that the contents of both NAPE and NAE increase in response to increased Ca^{2+} concentration, and it has been suggested that both of these lipids may have a role in cytoprotective response in various forms of neurotoxicity, whether mediated by their interaction with membranes or enzymes or mediated by the activation of cannabinoid receptors (*43*, *44*). In a recent study, it has been reported that in cultured mouse epidermal cells serum depravation leads to elevated levels of NAPEs and NAEs (*45*). In all such cases where an increase in the levels of NAPEs and NAEs is observed, the *N*-acyl chain is usually of 16−20 C atoms long, with C-16 and C-18 chains being the most predominant, and the major fraction of them are saturated, or mono- or diunsaturated (*1*, *44*, *45*). The *N*-acyl chains of the spin-labeled NAPEs used in the study presented here are all stearoyl (18 C atoms long) and are therefore rather similar to those found in endogenous NAPEs. The results of our ESR experiments, which demonstrate that the *N*-acyl chain of NAPE is located at the same vertical position as that of the *sn*-2 acyl chain, provide a structural basis for rationalizing these interesting biological properties exhibited by NAPEs.

CONCLUSIONS

The spin-label ESR studies reported here demonstrate that the C-18 *N*-acyl chain of *N*-acyl PE inserts directly in the hydrophobic interior of the membrane. The vertical location of the *N*-acyl chain, as probed by spin-label ESR, is comparable to that of the *sn*-2 acyl chains. Furthermore, the effect of cholesterol on the mobility and ordering of the *N*-acyl chains of *N*-acyl PE is qualitatively similar to that exerted by cholesterol on the *O*-acyl chains of other glycerophospholipids such as phosphatidylcholines. The high degree of compatibility of *N*-acyl PE with the bilayer environment of normal diacyl phospholipids supports the idea that NAPEs provide a suitable reservoir for the rather more membrane-disruptive NAEs that are only mobilized in response to membrane stress.[2] This does not exclude the possibility that other, less passive, effects of NAPEs, such as the enhancement of the hydrophobic permeation barrier and differences in detail in the interactions with cholesterol that are found here, may not also play a role in membrane bilayer stability.

REFERENCES

1. Schmid, H. H. O., Schmid, P. C., and Natarajan, V. (1990) *Prog. Lipid Res. 29*, 1−43.
2. Bomstein, R. A. (1965) *Biochem. Biophys. Res. Commun. 21*, 49−54.
3. Dawson, R. M. C., Clarke, N., and Quarles, R. H. (1969) *Biochem. J. 114*, 265−270.
4. Hazlewood, G. P., and Dawson, R. M. C. (1975) *Biochem. J. 150*, 521−525.
5. Matsumoto, M., and Miwa, M. (1973) *Biochim. Biophys. Acta 296*, 350−364.
6. Gray, G. M. (1976) *Biochim. Biophys. Acta 431*, 1−8.
7. Epps, D. E., Natarajan, V., Schmid, P. C., and Schmid, H. H. O. (1980) *Biochim. Biophys. Acta 618*, 420−430.
8. Natarajan, V., Schmid, P. C., Reddy, P. V., Zuzarte-Augustin, M. L., and Schmid, H. H. O. (1985) *Biochim. Biophys. Acta 835*, 426−433.
9. Natarajan, V., Reddy, P. V., Schmid, P. C., and Schmid, H. H. O. (1981) *Biochim. Biophys. Acta 664*, 445−448.
10. Reddy, P. V., Natarajan, V., Schmid, P. C., and Schmid, H. H. O. (1983) *Biochim. Biophys. Acta 751*, 241−246.
11. Schmid, H. H. O., Schmid, P. C., and Natarajan, V. (1996) *Chem. Phys. Lipids 80*, 133−142.
12. Devane, W. A., Hanus, L., Breuer, A., Pertwee, R. G., Stevenson, L. A., Griffin, G., Gibson, D., Mandelbaum, A., Etinger, A., and Mechoulam, R. (1992) *Science 258*, 1946−1949.
13. Facci, L., Toso, R. D., Romanello, S., Buriani, A., Skaper, S. D., and Leon, A. (1995) *Proc. Natl. Acad. Sci. U.S.A. 92*, 3376−3380.
14. Sugita, M., Williams, M., Dulaney, J. T., and Moser, H. W. (1975) *Biochim. Biophys. Acta 398*, 125−131.
15. Venance, L., Piomelli, D., Glowinski, J., and Giaume, C. (1995) *Nature 376*, 590−594.
16. Schuel, H., Goldstein, E., Mechoulam, R., Zimmerman, A. M., and Zimmerman, S. (1994) *Proc. Natl. Acad. Sci. U.S.A. 91*, 7678−7682.
17. Domingo, J. C., Mora, M., and de Madariaga, M. A. (1993) *Biochim. Biophys. Acta 1148*, 308−316.
18. Mercadal, M., Domingo, J. C., Bermudez, M., Mora, M., and De Madariaga, M. A. (1995) *Biochim. Biophys. Acta 1235*, 281−288.
19. Ambrosini, A., Bertoli, E., Mariani, P., Tanfani, F., Wozniak, M., and Zolese, G. (1993) *Biochim. Biophys. Acta 1148*, 351−355.
20. Epps, D. E., Schmid, P. C., Natarajan, V., and Schmid, H. H. O. (1979) *Biochem. Biophys. Res. Commun. 90*, 628−633.
21. Marsh, D., and Swamy, M. J. (2000) *Chem. Phys. Lipids 105*, 43−69.
22. Akoka, S., Tellier, C., LeRoux, C., and Marion, D. (1988) *Chem. Phys. Lipids 46*, 43−50.
23. Lafrance, D., Marion, D., and Pézolet, M. (1990) *Biochemistry 29*, 4592−4599.
24. Domingo, J. C., Mora, M., and de Madariaga, M. A. (1995) *Chem. Phys. Lipids 75*, 15−25.
25. Lafrance, C.-P., Blochet, J.-E., and Pezolet, M. (1997) *Biophys. J. 72*, 2559−2568.
26. Swamy, M. J., Marsh, D., and Ramakrishnan, M. (1997) *Biophys. J. 73*, 2556−2564.

27. Hitchcock, P. B., Mason, R., Thomas, K. M., and Shipley, G. G. (1974) *Proc. Natl. Acad. Sci. U.S.A. 71*, 3036−3040.
28. Buldt, G., Gally, H. U., Seelig, A., and Seelig, J. (1978) *Nature 271*, 182−184.
29. Marsh, D., and Watts, A. (1982) in *Lipid−Protein Interactions* (Jost, P. C., and Griffith, O. H., Eds.) Vol. 2, pp 53−126, Wiley-Interscience, New York.
30. Marsh, D. (1985) in *Spectroscopy and the Dynamics of Molecular Biological Systems* (Bayley, P. M., and Dale, R. E., Eds.) pp 209−238, Academic Press, London.
31. Marsh, D. (1982) in *Techniques in Lipid and Membrane Biochemistry* (Metcalfe, J. C., and Hesketh, T. R., Eds.) Vol. B4/II, pp B426/1−B426/44, Elsevier, Amsterdam.
32. Yeagle, P. L. (1993) in *Cholesterol in Membrane Models* (Finegold, L., Ed.) pp 1−12, CRC Press, Boca Raton, FL.
33. Sankaram, M. B., and Thompson, T. E. (1991) *Proc. Natl. Acad. Sci. U.S.A. 88*, 8086−8090.
34. Marsh, D. (1990) *Handbook of Lipid Bilayers*, pp 387, CRC Press, Boca Raton, FL.
35. Vist, M., and Davis, J. H. (1990) *Biochemistry 29*, 451−464.
36. Marsh, D. (1981) in *Membrane Spectroscopy. Molecular Biology, Biochemistry and Biophysics* (Grell, E., Ed.) Vol. 31, pp 51−142, Springer-Verlag, Berlin, Heidelberg, and New York.
37. Seelig, J. (1971) *J. Am. Chem. Soc. 93*, 5017−5022.
38. Marsh, D., and Watts, A. (1981) in *Liposomes: from Physical Structure to Therapeutic Applications* (Knight, C. G., Ed.) pp 139−188, Elsevier, North-Holland Biomedical Press, Amsterdam.
39. Knowles, A. F., Kandrach, A., Racker, E., and Khorana, H. G. (1975) *J. Biol. Chem. 250*, 1809−1813.
40. Basu, A., Prence, E., Garrett, K., Glew, R. H., and Ellingson, J. S. (1985) *Arch. Biochem. Biophys. 243*, 28−34.
41. Schmid, P. C., Reddy, P. V., Natarajan, V., and Schmid, H. H. O. (1983) *J. Biol. Chem. 258*, 9302−9306.
42. Chapman, K. D., Lin, I., and DeSouja, A. D. (1995) *Arch. Biochem. Biophys. 318*, 401−407.
43. Hansen, H. S., Lauritzen, L., Moesgaard, B., Strand, A. M., and Hansen, H. H. (1998) *Biochem. Pharmacol. 55*, 719−725.
44. Hansen, H. S., Moesgaard, B., Hansen, H. H., Schousboe, A., and Petersen, G. (1999) *Lipids 34*, S327−S330.
45. Berdyshev, E. V., Schmid, P. C., Dong, Z., and Schmid, H. H. O. (2000) *Biochem. J. 346*, 369−374.

BI000699L